14

Acoustic–Gravity Waves in the Ionosphere During Solar Eclipse Events

Petra Koucká Knížová and Zbyšek Mošna
Institute of Atmospheric Physic, Czech Academy of Sciences
Czech Republic

1. Introduction

Terrestrial atmosphere shows a high variability over a broad range of periodicities, which mostly consists of wave-like perturbations characterized by various spatial and temporal scales. The interest for short time variability in ionospheric attributes is related to the role that ionosphere plays in the Earth's environment and space weather. Acoustic-gravity waves (AGWs), waves in the period range from sub-seconds to several hours, are sources of most of the short-time ionospheric variability and play an important role in the dynamics and energetics of atmosphere and ionosphere systems. Many different mechanisms are likely to contribute to the acoustic-gravity wave generation: for instance, excitation at high latitudes induced by geomagnetic and consequent auroral activity, meteorological phenomena, excitation in situ by the solar terminator passages and by the occurrence of solar eclipses.
During solar eclipse, the lunar shadow creates a cool spot in the atmosphere that sweeps at supersonic speed across the Earth's atmosphere. The atmosphere strongly responds to the decrease in ionization flux and heating. The very sharp border between sunlit and eclipsed region, characterized by strong gradients in temperature and ionization flux, moves throughout the atmosphere and drives it into a non-equilibrium state. Acoustic-gravity waves contribute to the return to equilibrium. At thermospheric heights, the reduction in temperature causes a decrease in pressure over the totality footprint to which the neutral winds respond. Thermal cooling and downward transport of gases lead to neutral composition changes in the thermosphere that have significant influence on the resulting electron density distribution. Although the mechanisms are not well understood, several studies show direct evidence that solar eclipses induce wave-like oscillations in the acoustic-gravity wave domain.
Many different mechanisms are likely to contribute to wave generation and enhancement at ionospheric heights. Hence, it is difficult to clearly separate or differentiate each contributing agent and to decide which part of wave field belongs to the in situ generated and which part comes from distant regions. First experimental evidence of the existence of gravity waves in the ionosphere during solar eclipse was reported by Walker et al. (1991), where waves with periods of 30–33 min were observed on ionosonde sounding virtual heights.

1.1 Ionospheric sounding

As the solar radiation penetrates Earth's atmosphere it forms pairs of charged particles. Under a normal day-time conditions the ionization solar flux increases immediately after

sunrise, reaches maximum around local noon and decreases again till sunset. Under such conditions concentration of charged particles significantly grows in the atmosphere and forms atmospheric plasma called ionosphere. Due to the composition of the neutral atmosphere together with the changing efficiency of the incoming solar radiation, ionosphere is stratified into the layers denoted D, E, F1 and F2. After sunset, electrons and ions recombine rapidly in the D, E and F1 layer. Due to slower recombination processes of atomic ions that dominate at heights approximately above 150km altitude, F2 layer remains present all the night. Special stratification Es, sporadic E layer, occurs sometimes at heights of E layer (Davies, 1990).

Ionosphere significantly affects propagation of the electromagnetic waves. According to a frequency of the wave with respect to a concentration of the ionospheric plasma, wave propagates through the medium or it is reflected. Electromagnetic waves with frequency lower than plasma frequency of the particular plasma parcel are reflected, which allows to estimate plasma frequency. Higher frequency waves propagate through plasma. An instrument called ionosonde (or digisonde) transmits electromagnetic wave of a defined frequency and detects it after reflection from the ionosphere. Typical ionosonde sounding range is 1 MHz – 20 MHz. For each sounding wave ionosonde records time of flight τ on the path transmitter - reflection point – receiver. Time of flight is simply converted into a virtual height $h_{virtual} = \frac{\tau.c}{2}$ that corresponds to wave propagation in the vacuum (c stands here for speed of light). Virtual height is equal or higher than the corresponding real height. The output of the measurement is height-frequency characteristics called an ionogram. Real height electron concentration profiles can further be inverted from ionograms using for instance programs POLAN (Titheridge, 1985) or NHPC (Huang and Reinish, 1996). Ionosphere represents inhomogeneous and anisotropic medium which leads to a wave splitting into an ordinary and extraordinary wave modes. Hence, two reflection traces are recorded by the ionosonde (as seen on ionograms in Figure 1). However, the extraordinary mode is not further used for electron concentration profile inversion.

Figure 1 shows typical day-time and night-time ionograms recorded by a digisonde in the observatory Pruhonice. Together with the ionograms there are plots of the real height electron concentration derived by NHPC routine. On the day-time electron concentration profile, three ionospheric layers E, F1 and F2 are present while on the night-time profile there is only F2 layer detected by the ionosonde.

Sequences of ionograms are widely used for analyses of variability of atmospheric plasma ranging from detection of rapid changes with periods of minutes to the study of long-term trends.

2. Basic theory of AGWs in the Earth's atmosphere

Most of the wave-like oscillations in the atmosphere can be described/parametrized using basic acoustic-gravity wave theory in the atmosphere. Details can be found, for instance, in works of Davies (1990), Bodo et al. (2001), Hargreaves (1982), Yeh & Liu (1974) among others. Here, we show brief derivation of the dispersion relation that any wave motion of the AGW type must satisfy. In a plane-stratified, isothermal atmosphere under gravity that is constant with height, two frequency domains exist in the atmosphere where atmospheric waves can propagate, acoustic and gravity wave. Atmosphere represents compressible gas that once compressed and then released would expand and oscillate about its equilibrium state. Its oscillation frequency is known as an acoustic cut-off frequency

$$\omega_a = \frac{c}{2H} \tag{1}$$

where c is speed of sound

$$c = \sqrt{\gamma g H} \tag{2}$$

γ is the ratio of specific heats at constant pressure and constant volume, g is the gravitational acceleration, and H is the scale height. For diatomic gas γ ~ 1.4.

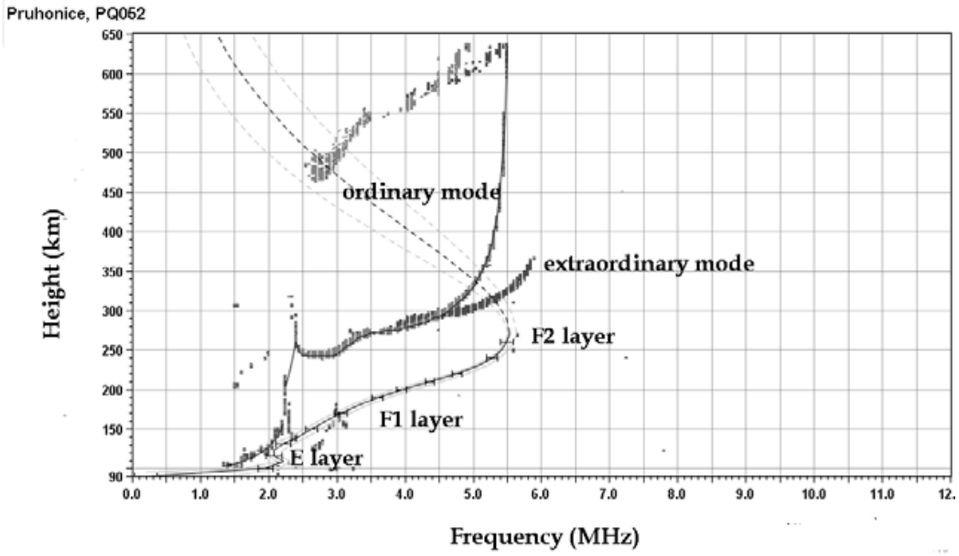

(a)

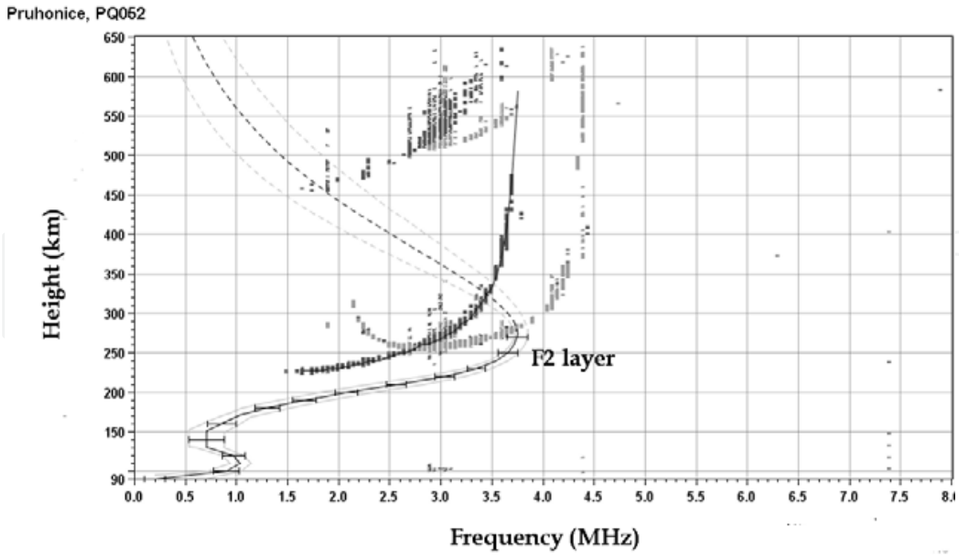

(b)

Fig. 1. Typical day-time (a) and night-time ionogram (b) measured by digisonde DPS 4 in the Observatory Pruhonice. On both plots, there is real hight electron concentration (solid line with error bars) provided as obtained by the NHPC routine.

Single element of fluid, parcel of the atmosphere, at height z with density ρ which is displaced in the vertical by Δz to a place where its density changes to ρ+Δρ, remains in pressure equilibrium with its surroundings. Displacement takes place adiabatically. This is valid when the motion is so slow that sound waves with speed

$$c = \sqrt{\frac{dp}{d\rho}} \tag{3}$$

where p stands for pressure can traverse the system faster than the time-scale of interest and the motion is so fast that the entropy is preserved. The parcel is no longer in equilibrium and starts to oscillate about its equilibrium height with buoyancy frequency.
The buoyancy force which acts on the parcel is balanced by inertial force (Newton's second law):

$$\rho \frac{d^2}{dt^2}(\Delta z) = -g\Delta\rho \tag{4}$$

where Δρ is the difference between internal and external densities.
Internal and external Δρ are derived as:

$$(\Delta\rho)_{internal} = \Delta p / c^2 = -\frac{g\rho}{c^2}\Delta z \tag{5}$$

which is due to compressibility of the fluid within the membrane and

$$(\Delta\rho)_{external} = -\frac{d\rho}{dz}\Delta z \tag{6}$$

is the change of background density at new position due to inhomogeneous nature of the atmosphere. Taking both the contributions of Δρ we get

$$\frac{d^2}{dt^2}(\Delta z) = \left(g\frac{d}{dz}(\ln\rho) + g^2/c^2 \right)\Delta z \tag{7}$$

which can be recast into

$$\frac{d^2}{dt^2}(\Delta z) + \omega_B^2 \Delta z = 0 \tag{8}$$

where

$$\omega_B^2 = -g\left(\frac{d}{dz}(\ln\rho) + g/c^2 \right) \tag{9}$$

If $\omega_B^2 > 0$, the solution is oscillatory and the fluid parcel will oscillate with characteristic buoyancy frequency ω_B called Brunt-Vaisala frequency.
More convenient form used for atmosphere is following:

$$\omega_B^2 = (\gamma - 1)g^2/c^2 + g/c^2 dc^2/dz \tag{10}$$

This approximation is valid in the atmosphere-ionosphere system of our interest.

In isothermal atmosphere ω_B reduces to

$$\omega_B^2 = (\gamma - 1) g^2 / c^2 \tag{11}$$

In the terrestrial atmosphere the buoyancy period depends on the height. The height variance of the acoustic cut-off and buoyancy frequencies in the isothermal atmosphere is shown in Figure 2.

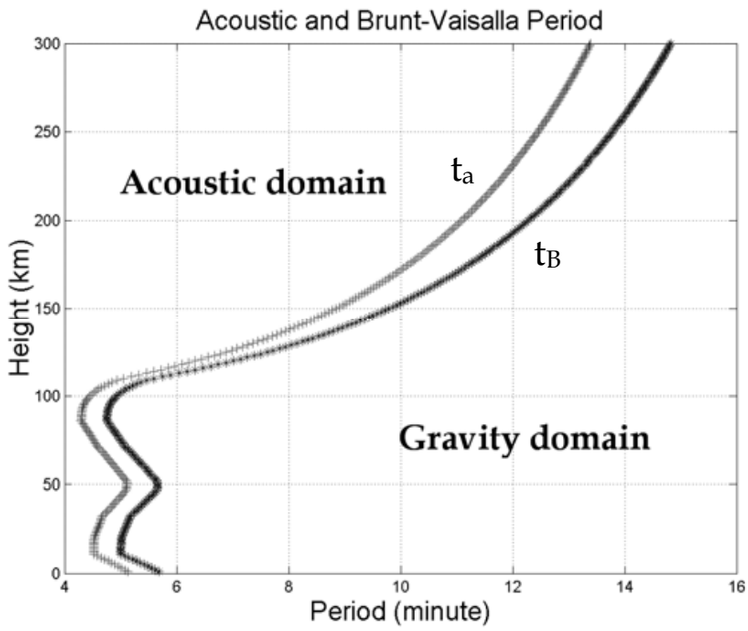

Fig. 2. Height dependence of acoustic cut-off period t_a and Brunt-Vaisala period t_B that represent limits dividing periods into acoustic and gravity wave domains. Period domain between acoustic cut-off and Brunt-Vaisala represents region where no AGW propagates.

Wave motion in the atmosphere can be described using mass conservation (continuity equation), and equation of motion:

$$\frac{\partial \rho}{\partial t} + \rho \nabla . \vec{u} + \left(\vec{u} . \nabla \right) \rho = 0 \tag{12}$$

$$\rho \left(\frac{\partial \vec{u}}{\partial t} + \left(\vec{u} . \nabla \right) \vec{u} \right) = -\nabla p + \rho g \tag{13}$$

where pressure gradients and gravity are the only forces causing the acceleration. Oscillation takes place adiabatically

$$\rho \left(\frac{\partial p}{\partial t} + \vec{u} . \nabla p \right) = \gamma p \left(\frac{\partial \rho}{\partial t} + \vec{u} . \nabla \right) \tag{14}$$

where ρ, p,γ and $\vec{u}$ are parameters of the atmosphere – density, pressure, ratio of specific heats, and velocity.

Applying the perturbation approach we are searching for wave-like solutions for the perturbation quantities. Further simplification comes from the assumption that the background state is of constant temperature T in which p_0/ρ_0 must be a constant.

$$p_0 / \rho_0 = c^2 / \gamma \tag{15}$$

Then the system (12), (13) and (14) reduces to:

$$\frac{\partial \rho'}{\partial t} + \rho_0 \vec{\nabla} . \vec{u'} - \rho_0 u_z / H = 0 \tag{16}$$

$$\rho_0 \frac{\partial \vec{u}}{\partial t} + \nabla p' - \rho' g = 0 \tag{17}$$

$$\rho_0 \left(\frac{\partial p'}{\partial t} - p_0 u_z' / H \right) = \gamma p_0 \left(\frac{\partial \rho'}{\partial t} - \rho_0 u_z' / H \right) \tag{18}$$

where index 0 denotes stationary (non fluctuating) component and the apostrophe denotes perturbation. These are the basic governing equations for the gravity waves. For a non-trivial solution the following prescription of the dispersion relation must be satisfied:

$$\omega^4 - \omega^2 \omega_a^2 - k_x^2 c^2 \left(\omega^2 - \omega_g^2 \right) - c^2 \omega^2 k_z^2 = 0 \tag{19}$$

From disperse relation, it is evident that between buoyancy frequency and acoustic cut-off frequencies one cannot have both k_x and k_z real. Figure 2 shows two period domains with border limits of acoustic cut-off period and buoyancy period.

An attenuation or growth in the wave amplitude must occur in either the vertical or the horizontal directions. We suppose that there is no variation in amplitude in horizontal directions so that k_x is purely real and k_z has an imaginary component. At frequencies exceeding acoustic cut-off ω_a, expression (19) becomes simple and the waves may be termed as ACOUSTIC WAVES. At frequencies smaller than Brunt-Vaisala frequency where gravity plays an important role, the waves are called GRAVITY or INTERNAL GRAVITY WAVES. Brunt-Vaisala frequency and acoustic cut-off frequency divide the frequency spectrum into two domains in which ω_g forms the high frequency limit for one class $\omega<\omega_g$ normally called internal gravity waves and ω_a is the low frequency limit for another class $\omega>\omega_a$ called the acoustic waves. A gap in the frequency spectrum exists between ω_g and ω_a where no internal waves can propagate.

Important approximations can be obtained under the assumption $|k_z| >> 1/2H$ and $\omega << \omega_g$ then:

$$k_z^2 = \left(\omega_g^2 / \omega^2 \right) k_x^2 \tag{20}$$

These approximations apply to much of the observed gravity waves. From (20) we see that the angle of ascent of the phase α is:

$$tg\alpha = k_z / k_x = \omega_g / \omega = \tau / \tau_g \tag{21}$$

The motions of the air parcels are, in general, ellipses in the plane of propagation and have components transverse to the direction of wave propagation. The ratio of the horizontal displacement ξ to its vertical displacement ζ is:

$$\frac{\xi}{\zeta}=\frac{\frac{ck_x}{\omega}}{\left(\frac{ck_x}{\omega}\right)^2-1}\left(\frac{ck_z}{\omega}-i\sqrt{\left(\frac{\omega_a}{\omega}\right)^2-\left(\frac{\omega_g}{\omega}\right)^2}\right) \tag{22}$$

On the frequencies just above the acoustic cutoff the air motion is essentially vertical. With acoustic waves on high frequencies the motion is radial as in sound waves. The motion is circular with horizontal propagation at a frequency $\omega_a\sqrt{2/\gamma}$. Gravity wave propagation is limited to angles between

$$\phi_{min}=\sin^{-1}\left(\frac{\omega}{\omega_g}\right)\ ,\ \phi_{max}=\pi-\sin^{-1}\left(\frac{\omega}{\omega_g}\right) \tag{23}$$

The sense of rotation of the air for gravity waves is opposite than for acoustic waves. As Φ approaches its asymptotic values the air motion becomes linear and transverse to the direction of propagation. Air parcel rotation is clockwise in case of acoustic waves while anticlockwise in case of gravity waves. Energy vector lies in the same quadrant as direction of propagation of acoustic waves. Energy flows up when phase travels down and vice versa in case of gravity waves propagation. This is important property since it accounts for the observed downward phase propagation when the source is below the level at which a disturbance is observed.

The horizontal u_x and vertical u_z components of the packet velocity are obtained from disperse relation:

$$u_x=\frac{c^2k_x\left(\omega^2-\omega_g^2\right)}{\omega\left(2\omega^2-\omega_a^2-c^2k^2\right)}$$
$$u_z=\frac{c^2k_z\omega^2}{\omega\left(2\omega^2-\omega_a^2-c^2k^2\right)} \tag{24}$$

Due to coupling between neutral and charged components the initial wave-like oscillation in the neutral atmosphere induces wave-like perturbation in the ionosphere. Perturbation in the ion production is the most effective when solar ionizing rays are nearly in alignment with the initial wave front. Perturbations in the neutral atmosphere may cause perturbations in chemical processes. Presence of AGW influences the ionisation rate through changes in the local neutral density and temperature, and through changes in the ionisation radiation absorption (Hooke, 1970).

3. AGW in the ionospheric plasma

Acoustic-gravity waves are always present in the Earth's atmosphere. AGWs arise from many natural sources like convection, topography, wind shear, moving solar terminator, earthquakes, tsunami, etc. Increase in wave-like activity is associated also with human

activity including coordinated experiments or unwilling accidents. AGWs influence on the upper atmosphere is not yet understood enough. They produce a great amount of variability and contribute to the background conditions in a specific parcel of the atmosphere. Gravity waves propagating from lower laying atmosphere have been long regarded as a very important source of the energy and momentum transfer in the upper atmosphere (Hines, 1960). The breaking of the upward propagating waves affects wind system, generates turbulence and heats the atmospheric gas.

Waves that reach upper atmosphere produce travelling atmospheric disturbances (TAD) or travelling ionospheric disturbances (TID) and even form the ionospheric inhomogenities which grow and finally break into the plasma instabilities observed by radar techniques that might cause scintillation of the communication signals propagating through the ionosphere. From the observation it is evident that the thermosphere is continuously swept by the acoustic-gravity waves. Statistically, the waves show a moderate preference for southward travel, with this preference being reduced or shifted to southeastward travel during disturbed times (Oliver et al., 1997). Experimental studies show that AGW activity in the ionosphere slightly increases during dawn and dusk periods of the day (Galushko et al., 1998; Somsikov & Ganguly, 1995; Sauli et al., 2005 among others). Influence of infrasonic waves generated by ground experimental sources on the ionosphere was reported for instance by Rapoport et al. (2004).

Solar eclipse represents well defined source of the AGW in the atmosphere and ionosphere systems. During solar eclipse event, solar ionization flux decreases producing well-defined cool spot in the atmosphere that moves through the Earth's atmosphere. Moving source in the atmosphere can emit both acoustic and gravity waves. Supersonic motion of the source forms wave field with bow wave. Both acoustic and gravity waves can be radiated in association with supersonic motion in the atmosphere. When the source is moving within atmosphere with subsonic velocity only gravity waves can be emitted (Kato et al., 1977).

4. Solar eclipse event – signatures in the ionospheric plasma

It has been proposed by Chimonas and Hines (1970) that solar eclipses can act as sources for AGWs. The lunar shadow creates a cool spot in the atmosphere that sweeps at supersonic speed across the Earth. The sharp border between sunlit and eclipsed regions, characterized by strong gradients in temperature and ionization flux, moves throughout atmosphere and drives it into a non-equilibrium state. Earth atmosphere shows variable sensitivity to the changes of ionization flux.

4.1 Experiments

Solar eclipse event represents phenomenon that can be precisely predicted, hence many observational campaigns are organised around the world. Effects of the solar eclipses on the ionospheric plasma are studied by mean of GPS techniques, radars, vertical ionospheric soundings etc. Study limitations lay mainly in the fact that there are no identical solar eclipse events. Moreover, solar eclipse induced effects are easily to be mixed with effects caused by geomagnetic field variations, diurnal changes of the ionosphere, seasonal variability of the atmosphere/ionosphere etc. In the upper atmosphere, AGWs can be observed either directly as neutral gas fluctuations or indirectly as induced ionospheric

plasma variations. Despite intensive research many questions in the problem of the generation and propagation remain to be understood.
Studies by Fritts and Luo (1993) suggest that perturbations generated by the eclipse induced ozone heating interruption may propagate upwards into the thermosphere–ionosphere system where they have an important influence. Temperature fluctuations and electron density changes propagate as a wave, away from the totality path, cf. Muller-Wodarg et al. (1998). By means of vertical ionospheric sounding, Liu et al. (1998) detected waves excited during solar eclipse event at F1 layer heights and their generation and/or enhancement attributed to changes of temperatures and variations of the height of the transition level for the loss coefficient and the height of the peak of electron production. Studies reported by Farges et al. (2001) suggest a longitudinal diversity of the disturbances with respect to pre-noon and postnoon phases. Xinmiao et al. (2010) reported synchronous oscillations in the Es and F layer during the recovery phase of the solar eclipse. Ivanov et al. (1998) found that during solar eclipse with maximum obscuration of about 70% the F-region electron density decreased by 6-8% compared to a control day and detected travelling ionospheric disturbances. Additionally, they detected strong variations in the difference group delays with a period about 40 minutes associated with the start and end of the eclipse. Oscillations in the ionosphere, similar to gravity waves, were observed following some solar eclipse events (Chimonas and Hines, 1970; Cheng et al., 1992; Liu et al., 1998; Sauli et al., 2006). Investigation of the latitudinal dependence of NmF2 (the maximum electron density of the F2 layer) indicated that the strongest response was at middle latitudes (Le et al., 2009). The response of the sporadic-E (Es) layer also differed in each solar eclipse event. A remarkable decrease in Es layer ionization was observed during the eclipse of 20 July 1963 (Davis et al., 1964). Enhancement of Es layer ionization has also been reported and it has been suggested that it is related to internal gravity waves generated in the atmosphere during the solar eclipse (Datta, 1972).

4.2 Processes induced by solar eclipse

During the solar eclipse, on the time scale shorter than day-night change, the ionosphere reconfigures itself into a state similar to that of night situation. Photochemical ionization falls heavily almost to a night-time level. With the decreasing solar flux, atmospheric temperature falls in the moon shadow creating a cool spot with well defined border. Then the increasing solar flux starts ionization processes and warms the atmosphere again to daytime level.
Such changes in the ionization cause variation in the reflection heights, decrease/increase in electron concentration at all ionospheric heights, decrease/increase in the total electron content, rising/falling of the layer height. Such effects are characteristic for the processes during sunrise/sunset in the ionosphere. However, supersonic movement of the eclipsed region represents a key difference from the regular solar terminator motion at sunrise and sunset times. These changes in the neutral atmosphere and ionosphere induced by solar eclipse force the evolution of the ionospheric plasma toward a new equilibrium state. The return to equilibrium is likely accompanied by the eclipse induced wave motions excited in the atmosphere. Any moving discontinuity of gas parameters such as temperature, pressure etc. will generate transit-like waves. In the upper ionosphere, waves can be generated by a strong horizontal electron pressure gradient. Possible mechanisms contributing to the wave generation in the region of solar terminator are in detail discussed by Somsikov & Ganguly (1995).

Solar eclipse induces changes in all atmospheric regions extend from the upper atmosphere down to ground level. Despite the low magnitude of the eclipse induced effects at ground level, Jones et al. (1992) reported wave-like oscillation related to eclipse on the microbarometer pressure records. The cooling effect of the Moon's shadow may induce the powerful meridional airflow in the atmosphere, which accelerates the ionized clouds in the Es layer and forms the wind shear to raise the observed Doppler frequency shift and foEs values, respectively (Chen et al., 2010).

5. Solar eclipse observed by vertical ionospheric sounding in midlatitudes

Vertical sounding measurements provide local information on the electron density distribution of the bottomside ionosphere. Electron concentration in the plasma and its corresponding plasma frequency are related via following equation:

$$f_p^2 = \frac{Ne^2}{4\pi\varepsilon_0 m} \tag{25}$$

where f_p denotes plasma frequency and N, e, ε_0 and m stand for the electron concentration, the charge of electron, permittivity of free space, and the mass of the electron, respectively.

This section summarizes experimental results from the midlatitude ionospheric observatory Pruhonice (50N, 15E). At the observatory, the vertical sounding measurements were performed with ionosonde IPS 42 KEL Aerospace till the end of year 2003. Then this older equipment was replaced by digisonde DPS 4. Special campaigns of rapid sequence soundings were organized in order to study in detail ionospheric behavior during partial solar eclipses of 11 August 1999, 4 January 2011 and annular solar eclipse 3 October 2005. All three analyzed events were characterized by low geomagnetic activity; hence they represent a good occasion to observe mostly solar eclipse induced effects in the ionosphere. However, inconclusive results of the solar eclipse observations rise from the fact that different solar eclipses produce different plasma motions. Indeed, the travel cone geometry and its angular effects on the magnetized plasmas are different for each eclipse.

Solar eclipse of 11 August 1999 (as a total seen in place as close as 200 km from the measurement point) represents so far the event of the highest solar disc coverage observed in the Observatory Pruhonice. Figure 3 depicts sequence of raw ionograms measured during this event by IPS 42 KEL Aerospace equipment. The ionograms were recorded with the cadence of 1 minute. On the ionograms there is clearly seen that the eclipse event affects whole electron density profile. Critical frequencies in the E and F layer decrease before maximum disc occultation and then increase again. The electron density decrease in the E layer is much stronger than in the F layer due to different dominant type of the recombination. Electron density fall and increase occur simultaneously with occultation and de-occultation of the solar disc in the E and F1 layer while the F2 layer electron density reacts with slight delay. There are special structures of the spread F type developed on the profile after beginning of the solar disc occultation (clearly seen on ionograms at 9.14 UT and 9.16 UT). Shape of the F layer is affected as well. Unfortunately, effects in the F1 region cannot be discussed here in details because F1 layer is blanketed by strong sporadic E layer during part of the solar eclipse.

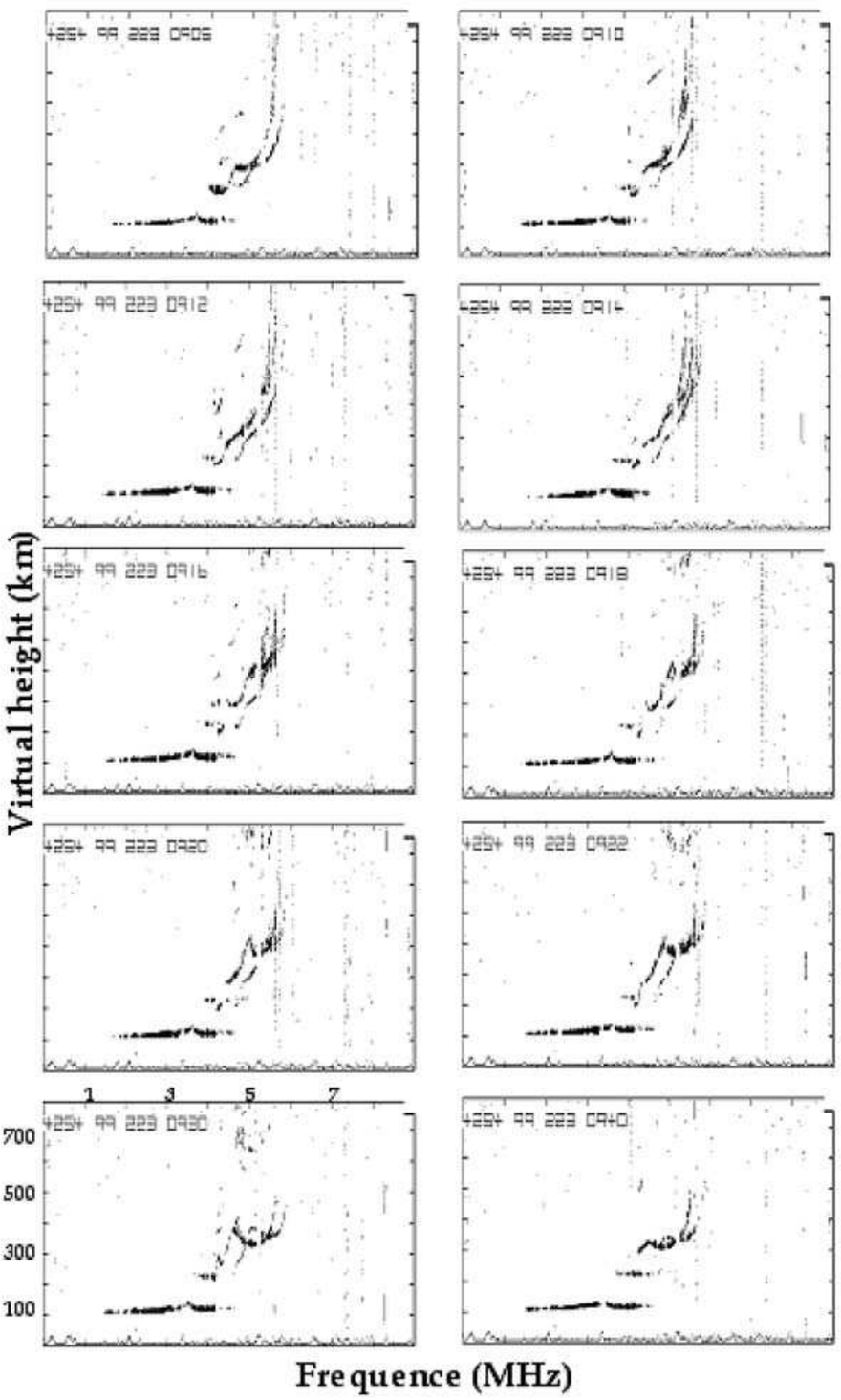

Fig. 3. Sequence of raw ionograms measured by the ionosonde KEL Aerospace IPS 42 at the observatory Pruhonice. During the special campaign ionograms were recorded with one-minute resolution in order to study rapid ionospheric changes during the solar eclipse.

Detail analysis of electron concentration by mean of spectral analysis reveals that within oscillation of electron concentration there occur several clear wave-like oscillations. It has been shown by Sauli et al. (2007) that wavelet spectral analysis is very convenient approach for such wave detection. The advantage of the wavelet based analysis is identification of the structure occurrence time which helps to associate particular wave-like structure to the agent. Figure 4 shows estimated wave parameters for selected structure that is coherent through all studied heights. Parametrization of the wave-like structure is based on AGW approximation described in Section 2. From Figure 4 it is evident that wave originates at height of about 200 km and propagates upward and downward from the source region.

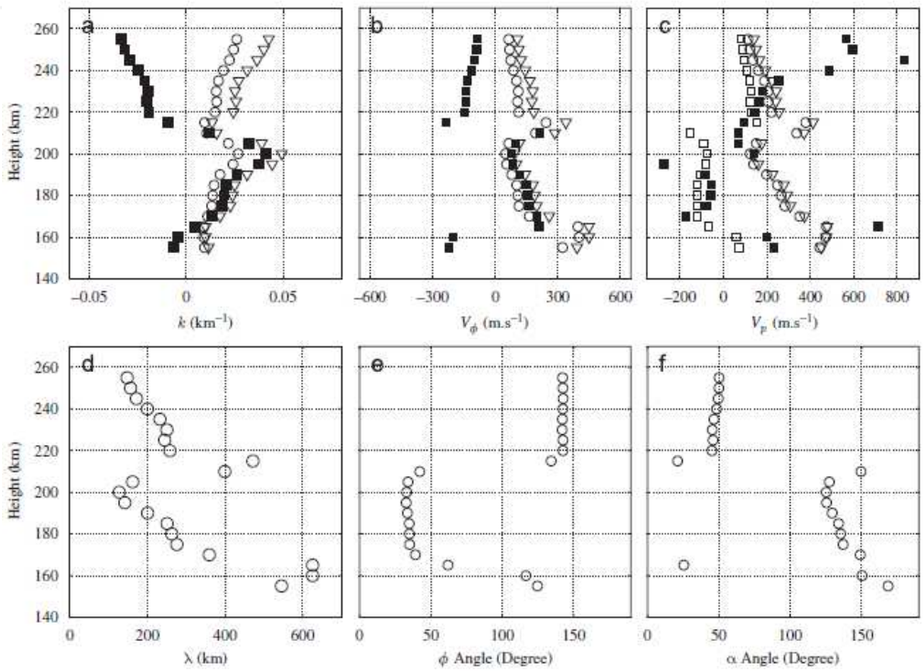

Fig. 4. Parameters of acoustic-gravity wave structure detected within ionospheric plasma during solar eclipse event 11 August 1999 (Sauli et al., 2007). Panels: wave vector (a), phase velocity (b), packet velocity (c), wave number (d), energy (e) and phase (f) angles. For the vectors of first row, the '□' correspond to the measured (full squares) and computed (empty symbols) z-components, the '○' correspond to the horizontal components while the '▽' are related to the modulus.

Another representation of the rapid changes in the ionospheric plasma is shown on the profilogram (Figure 5) measured during solar eclipse 3 October 2005 by DPS 4. Decrease in the plasma frequency at all heights is well developed. Within plasma frequency oscillation, several wave coherent structures were found that can be attributed to the eclipse event. These structures occur in the plasma at the maximum of the eclipse and after the event. In all cases we detected a component of upward energy progression. Due to the occurrence time and low geomagnetic activity the detected wave-like oscillations in the ionospheric plasma are likely signatures of bow shock and possibly waves excited by cooling of ozone in the lower laying atmosphere. Estimated velocities for one particular structure are shown in Figure 6.

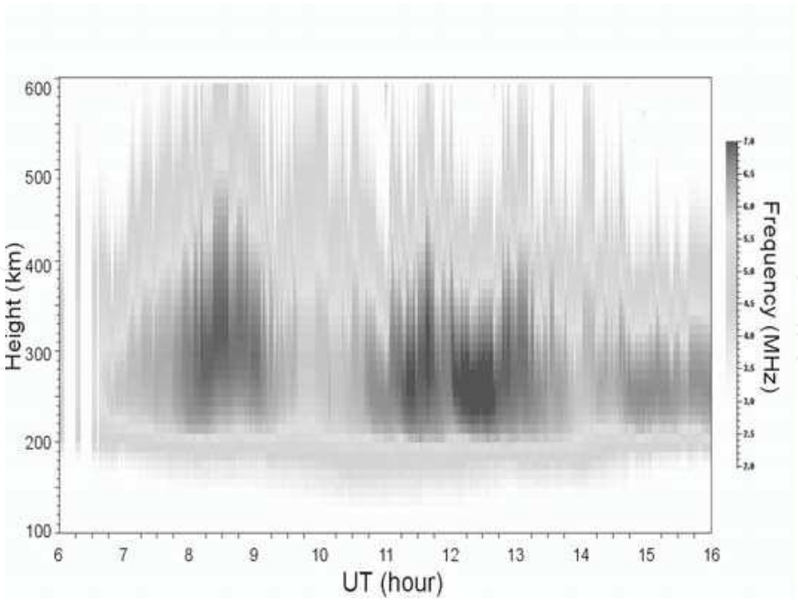

Fig. 5. Profilogram (height-time-plasma frequency development) during solar eclipse 3 October 2005 as measured by DPS 4. Ionograms were measured every 2 minutes. All ionograms were manually scaled and inverted into true-height profiles using True Height Profile Inversion Tool NHPC.

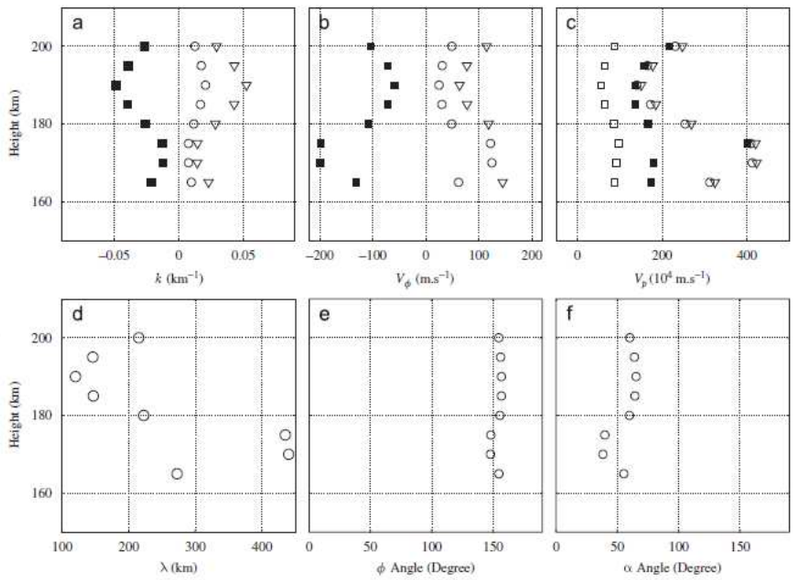

Fig. 6. Parameters of acoustic-gravity wave structure detected within ionospheric plasma during solar eclipse event 3 October 2005 (Sauli et al. 2007). Panels: wave vector (a), phase velocity (b), packet velocity (c), wave number (d), energy (e) and phase (f) angles. For the vectors of first row, the '□' correspond to the measured (black) and computed (empty) z-components, the '○' correspond to the horizontal components while the '▽' are related to the modulus.

Result of the annular eclipse is significantly different from the case of the total eclipse event of 1999 where the dominant AGW activity took place at the beginning of eclipse. The atmospheric cooling and decrease in radiation flux during an annular solar eclipse is not as strong as during a total eclipse and the ionospheric response occurs with time delay.

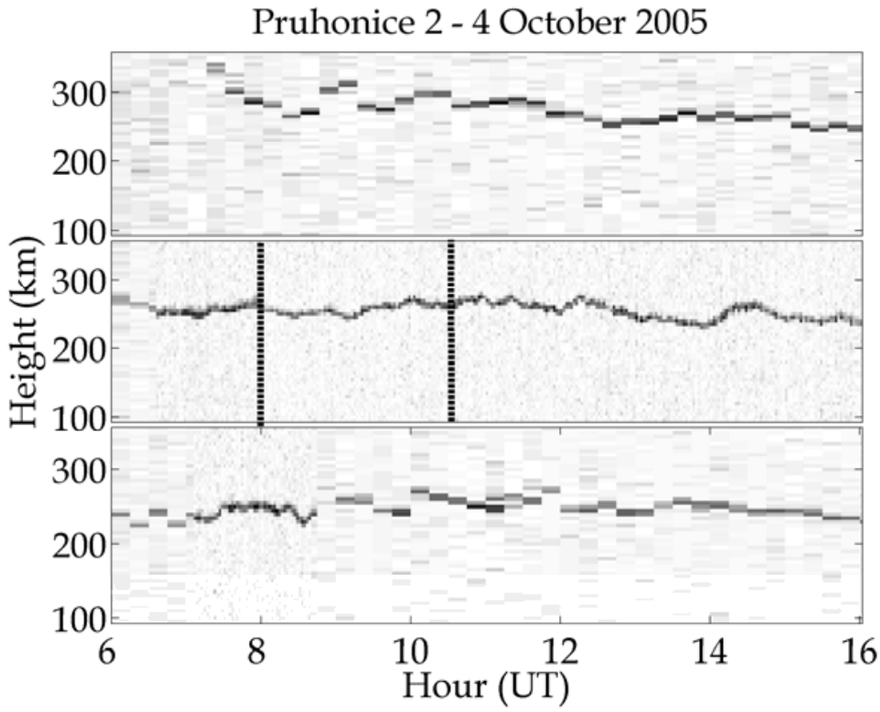

Fig. 7. Virtual reflection heights of plasma frequency in the range 4.2 - 4.3 MHz derived from raw ionograms. From up to bottom: day before, day of eclipse, day after eclipse. Vertical lines in middle panel depict beginning and end of the eclipse. Time resolution is different for day of solar eclipse (2 min) and days before/after (15 min).

In Figure 7 and Figure 8, there are plots of virtual reflection height variations at single frequency during three consecutive days, day of solar eclipse event and one day before and after the event. Variation of the reflection height during eclipse event of 3 October 2005 does not differ much from the corresponding variation during reference time span day before and day after. Wave-like oscillations excited by solar eclipse are of comparable magnitude as those induced by other sources preceding and consecutive day. On the contrary, clear difference in reflection height oscillation during reference days and solar eclipse event is perfectly seen in Figure 8. Records of virtual heights at fixed frequency from January 4, 2011 present strong ionospheric response which is exhibited as periodic changes in reflection height. Sharp changes in the reflection height develop immediately after the beginning of the solar disc occultation and last till the end of eclipse event. Higher wave-like activity remains remarkable whole day. In this partial solar eclipse event, wave-like oscillations can be very probably attributed to the solar eclipse.

Strong decrease in electron concentration in practically whole electron profile as well as the wave-like changes were observed during and after August 11, 1999 and January 4, 2011. Wave-like activity develops immediately after the start of the solar disc obscuration during

partial solar eclipse. During annular solar eclipse, significant acoustic-gravity wave type bursts develop around and after maximum phase of the eclipse.

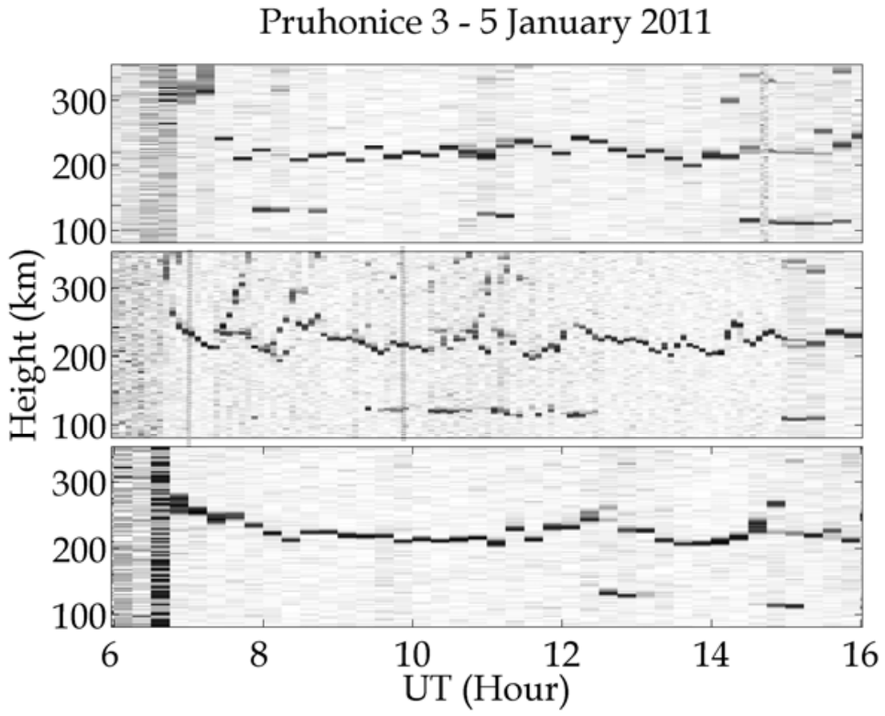

Fig. 8. Virtual reflection heights of plasma frequency range 3.4 – 3.5 MHz derived from raw ionograms. From up to bottom: day before, day of eclipse, day after eclipse. Vertical lines in middle panel depict beginning and end of the eclipse. Time resolution is different for day of solar eclipse (5 min) and days before/after (15 min).

6. Conclusion

Acoustic-Gravity waves play important role in the dynamic of the upper atmosphere. Vertical ionospheric sounding represents powerful tool that allows us to monitor acoustic-gravity wave activity in the ionosphere. Ionospheric observation of such a strong event as solar eclipse gives us an opportunity to better understand processes of creation and dissipation of the AGW in the area of the ionosphere. Although the acoustic-gravity waves are always present in the area of our interest, sharp temporally well-defined changes of solar flux during the solar eclipse give us a possibility to define sources of AGW.

It is rather uneasy to unambiguously assess causality between the solar eclipse events and the detected wave structures in the ionospheric plasma. Difficulties result from the fact that there are no two exactly identical solar eclipse events and from limitations of sounding techniques. Despite the fact that various AGW sources have been identified, many others remain to be found. Amongst irregular AGW bursts, regular increase in AGW activity were found to occur around sunrise and sunset hours, excited by Solar Terminator movement. Most of other sources (meteorological systems, geomagnetic and solar disturbances, etc.) and corresponding wave-like oscillations contribute to the irregular patterns of AGW activity observed in the ionospheric plasma.

As the solar eclipses, analyzed in the Section 5, occur sufficiently long time after the sunrise hours, one can assume that none of the reported waves are induced by solar terminator. During the analyzed sounding campaigns, no wave coming from auroral zone was expected, due to the quiet geomagnetic and solar activity. Additionally, meteorological analysis shows that meteorological systems very probably did not influence the ionosphere during studied events by means of AGW. The acoustic-gravity wave activity increases after a notably larger delay for the annular solar eclipse compared to the total solar eclipses: waves are found during the maximum phase of the eclipse only for the former while they occur during the initial phase for the latter. This discrepancy in gravity waves generation/occurrence can likely be explained by differences in the terrestrial atmosphere cooling: the border between sunlit and eclipsed region is much sharper in the case of total eclipse. Analyzing wave propagations, we observe predominantly upward propagating structures. The wave structure, that propagate upward and downward from the source region located around 200 km height, was created during an exceptional case related to the Solar eclipse of 11 August 1999.

7. References

Altadill, D., Sole, J.G. & Apostolov, E.M. (2001). Vertical structure of a gravity wave like oscillation in the ionosphere generated by the solar eclipse of August 11, 1999. *Journal of Geophysical Research*, 106 (A10), 21419–21428, ISSN 0148-0227.

Bodo, G., Kalkofen, W., Massaglia, S. & Rossi, P. (2001). Acoustic waves in a stratified atmosphere. III. Temperature inhomogenities. *Astronomy & Astrophysics*, 370, pp. 1088-1091, ISSN 0004-6361.

Chen, G., Zhao, Z., Zhou, C., Yang, G. & Zhang, Y. (2010). Solar eclipse effects of 22 July 2009 on Sporadic-E. *Annales Geophysicae*, 28, 353–357, ISSN 0992-7689.

Cheng, K., Huang, Y.N. & Chen, S.W. (1992). Ionospheric effects of the solar eclipse of September 23, 1987, around the equatorial anomaly crest region. *Journal of Geophysical Research*, 97, A1, 103–111. ISSN 0148-0227.

Chimonas, G. & Hines, C.O. (1970). Atmospheric gravity waves induced by a solar eclipse. *Journal of Geophysical Research,* 75, 4, pp. 875, ISSN 0148-0227.

Datta, R.N. (1972). Solar-eclipse effect on sporadic-E ionization. *Journal of Geophysical Research*, 77, 1, 260–262.

Davies, K. (1990). *Ionospheric radio.* Peter Peregrinus Ltd., ISBN 0 86341 186 X, London, United Kingdom.

Davis, J.R., Headrick, W.C. & Ahearn, J.L. (1964). A HF backscatter study of solar eclipse effects upon the ionosphere. *Journal of Geophysical Research*, 69 (1), 190–193. ISSN 0148-0227.

Farges, T., Jodogne, J.C., Bamford, R., Le Roux, Y., Gauthier, F., Vila, P.M., Altadill, D., Sole, J.G. & Miro, G. (2001). Disturbances of the western European ionosphere during the total solar eclipse of 11 August 1999 measured by a wide ionosonde and radar network. *Journal of Atmospheric and Solar-Terrestrial Physics,* 63, 9, pp. 915–924, ISSN 1364-6826.

Fritts, D.C. & Luo, Z. (1993). Gravity wave forcing in the middle atmosphere due to reduced ozone heating during a solar eclipse. *Journal of Geophysical Research*, 98, pp. 3011–3021, ISSN 0148-0227.

Galushko, V.G., Paznukhov, V.V., Yampolski, Y.M. & Foster, J.C. (1998). Incoherent scatter radar observations of EGW/TID events generated by the moving solar terminator. *Annales Geophysicae*, 16, pp. 821-827, ISSN 0992-7689.

Hargreaves, J.K. (1982). The upper atmosphere and solar-terrestrial relations. An introduction to the aerospace environment. Van Nostrand Reinhold, ISBN 0 521 32748 2, Cambridge, United Kingdom.

Hines, C.O. (1960). Internal atmospheric gravity waves at ionospheric heights. Canadian Journal of Physics, 38, pp. 1441–1481, ISSN 1208-6045.

Hooke, W.H. (1968). Ionospheric irregularities produced by internal atmospheric gravity waves. *Journal of Atmospheric and Solar-Terrestrial Physics,* 30, pp. 795-829, ISSN 1364-6826.

Huang X. & Reinish B.W (1996). Vertical electron density profiles from the digisonde network. *Advances in Space Research.*, 18, pp. 121□129, ISSN 0273-1177.

Ivanov, V.A., Ryabova, N.V., Shumaev, V.V., Uryadov, V.P., Nosov, V.E., Brinko, I.G. & Mozerov, N.S. (1998). Effects of the solar eclipse of 22 July 1990 at mid-latitude path of HF propagation. *of Atmospheric and Solar-Terrestrial Physics,* 60, 10, pp. 1013-1016, ISSN 1364-6826.

Jones, B.W., Miseldine, G.J. & Lambourne, R.J.A. (1992). A possible atmospheric-pressure wave from the total solar eclipse of 22 July 1990. *Journal of Atmospheric and Terrestrial Physics,* 54, 2, pp.113-115, ISSN 1364-6826.

Kato, S., Kawakami, T. & St. John, D. (1977). Theory of gravity wave emission from moving sources in the upper atmosphere. *Journal of Atmospheric and Terrestrial Physics,* 39, pp. 581–588, ISSN 1364-6826.

Le, H., Liu, L., Yue, X., Wan, W. & Ning, B. (2009). Latitudinal dependence of the ionospheric response to solar eclipses. *Journal of Geophysical Research,* 114, A07308, ISSN 0148-0227.

Liu, J.Y., Hsiao, C.C., Tsai, L.C., Liu, C.H., Kuo, F.S., Lue, H.Y. & Huang, C.M. (1998). Vertical phase and group velocities of internal gravity waves derived from ionograms during the solar eclipe of 24 October 1995. *Journal of Atmospheric and Solar-Terrestrial Physics,* 60, pp. 1679–1686, ISSN 1364-6826.

Muller-Wodarg, I.C.F., Aylward, A.D. & Lockwood, M. (1998). Effects of a mid-latitude solar eclipse on the thermosphere and ionosphere - a modeling study. *Geophysical Reseach Letters,* 25, 20, pp. 3787–3790, ISSN 0094-8276.

Oliver, W.L., Otsuka, Y., Sato, M., Takami, T. & Fukao, S. (1997). A climatology of F region gravity wave propagation over the middle and upper atmosphere radar. *Journal of Geophysical Research,* 102, A7, pp.14,499-14,512, ISSN 0148-0227.

Rapoport, V.O., Bespalov, P.A., Mityakov, N.A., Parrot, M. & Ryzhov, N.A. (2004). Feasibility study of ionospheric perturbations triggered by monochromatic infrasonic waves emitted with a ground-based experiment. *Journal of Atmospheric and Solar-Terrestrial Physics,* 66, pp. 1011-1017, ISSN 1364-6826.

Reinisch, B.W., Huang, X., Galkin, I.A., Paznukhov, V. & Kozlov, A. (2005). Recent advances in real-time analysis of ionograms and ionospheric drift measurements with digisondes, Journal of Atmospheric and Solar-Terrestrial Physics 67, pp. 1054-1062, ISSN 1364-6826.

Sauli, P., Abry, P., Boska, P. & Duchayne, L. (2006). Wavelet characterisation of ionospheric acoustic and gravity waves occuring during solar eclipse of August 11, 1999. *Journal of Atmospheric and Solar – Terrestrial Physics,* 68, pp. 586-598, ISSN 1364-6826.

Sauli, P., Roux, S.G., Abry, P. & Boska, J. (2007). Acoustic–gravity waves during solar eclipses: Detection and characterization using wavelet transforms. *Journal of Atmospheric and Solar-Terrestrial Physics,* 69, pp. 2465–2484, ISSN 1364-6826.

Sauli, P., Abry, P., Altadill, D. & Boska, P. (2005). Detection of the wave-like structures in the F-region electron density: two station measurement. *Studia Geophysica & Geodetica*, 50, pp. 131-146, ISSN 0039-3169.

Somsikov, V.M. & Ganguly, B. (1995). On the formation of atmospheric inhomogenities in the solar terminator region. *Journal of Atmospheric and Solar – Terrestrial Physics,* 57, 12, pp. 1513-1523, ISSN 1364-6826.

Titheridge J.E., 1985. Ionogram Analysis with the Generalised Program POLAN. *UAG Report-93*, 1985 (http://www.ips.gov.au/IPSHosted/INAG/uag_93/uag_93.html).

Walker, G.O., Li, T.Y.Y., Wong, Y.W., Kikuchi, T. & Huang, Y.N. (1991). Ionospheric and Geomagnetic effects of the solar eclipse of 18 march 1988 in East-Asia. *Journal of Atmospheric and Solar – Terrestrial Physics,* 53, 1–2, pp. 25–37, ISSN 1364-6826.

Xinmiao, Z., Zhengyu, Z., Yuannong, Z. & Chen, Z. (2010). Observations of the ionosphere in the equatorial anomaly region using WISS during the total solar eclipse of 22 July 2009. *Journal of Atmospheric and Solar – Terrestrial Physics,* 72, pp. 869–875, 1364-6826.

Yeh, K.C. & Liu, C.H. (1974). Acoustic-gravity waves in the upper atmosphere. *Reviews of Geophysics and Space Physics*, 12, 2, pp. 193-216, ISSN 8755-1209.

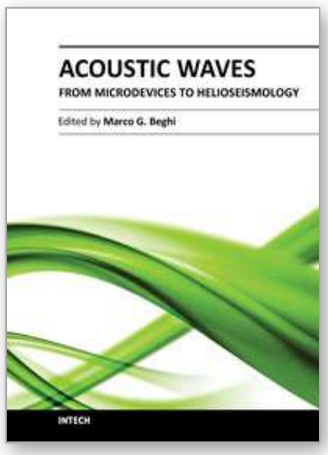

Acoustic Waves - From Microdevices to Helioseismology

Edited by Prof. Marco G. Beghi

ISBN 978-953-307-572-3
Hard cover, 652 pages
Publisher InTech
Published online 14, November, 2011
Published in print edition November, 2011

The concept of acoustic wave is a pervasive one, which emerges in any type of medium, from solids to plasmas, at length and time scales ranging from sub-micrometric layers in microdevices to seismic waves in the Sun's interior. This book presents several aspects of the active research ongoing in this field. Theoretical efforts are leading to a deeper understanding of phenomena, also in complicated environments like the solar surface boundary. Acoustic waves are a flexible probe to investigate the properties of very different systems, from thin inorganic layers to ripening cheese to biological systems. Acoustic waves are also a tool to manipulate matter, from the delicate evaporation of biomolecules to be analysed, to the phase transitions induced by intense shock waves. And a whole class of widespread microdevices, including filters and sensors, is based on the behaviour of acoustic waves propagating in thin layers. The search for better performances is driving to new materials for these devices, and to more refined tools for their analysis.

InTech Europe
University Campus STeP Ri
Slavka Krautzeka 83/A
51000 Rijeka, Croatia
Phone: +385 (51) 770 447
Fax: +385 (51) 686 166
www.intechopen.com

InTech China
Unit 405, Office Block, Hotel Equatorial Shanghai
No.65, Yan An Road (West), Shanghai, 200040, China
中国上海市延安西路65号上海国际贵都大饭店办公楼405单元
Phone: +86-21-62489820
Fax: +86-21-62489821

IntechOpen